Chinese Chemical Letters 30 (2019) 867–870

Contents lists available at ScienceDirect

Chinese Chemical Letters

journal homepage: www.elsevier.com/locate/cclet

Communication

Improvement of low-temperature catalytic activity over hierarchical Fe-Beta catalysts for selective catalytic reduction of NO_x with NH_3

Na Zhu[a,b,1], Zhihua Lian[a,1], Yan Zhang[a,c], Wenpo Shan[a,c,*], Hong He[a,b,c,d]

[a] Center for Excellence in Regional Atmospheric Environment and Key Laboratory of Urban Pollutant Conversion, Institute of Urban Environment, Chinese Academy of Sciences, Xiamen 361021, China
[b] University of Chinese Academy of Sciences, Beijing 100049, China
[c] Ningbo Urban Environment Observation and Research Station-NUEORS, Institute of Urban Environment, Chinese Academy of Sciences, Ningbo 315800, China
[d] State Key Joint Laboratory of Environment Simulation and Pollution Control, Research Center for Eco-Environmental Sciences, Chinese Academy of Sciences, Beijing 100085, China

ARTICLE INFO

Article history:
Received 27 January 2019
Received in revised form 1 March 2019
Accepted 5 March 2019
Available online 7 March 2019

Keywords:
Hierarchical structure
Fe-Beta
NH_3-SCR
Low-temperature activity
Kinetics

ABSTRACT

Hierarchical Fe-Beta obtained by hydrothermal synthesis exhibited higher low-temperature NH_3-SCR activity than conventional Fe-Beta. In order to identify the main factors leading to the difference in catalytic activity, we investigated the pore structure, acidity and Fe sites of the hierarchical Fe-Beta and conventional Fe-Beta. The enhanced activity of hierarchical Fe-Beta was mainly due to the increase of the quantity of active Fe species. NH_3-TPD and DRIFTS results of NH_3 adsorption clearly verified that hierarchical Fe-Beta had more Lewis acid sites, which is beneficial to the adsorption and activation of NH_3. The H_2-TPR, UV–vis DRS, and EPR results confirmed that the hierarchical Fe-Beta had more isolated active Fe species, which may be associated with that the hierarchical structure introduced more structural defects as ion-exchange sites. Based on the analysis of kinetics experiments and the above-mentioned characterizations, it can be concluded that the improvement of NH_3-SCR activity was not due to an intrinsic effect of the specific structural characteristics, but was related to more Fe active sites and better dispersion of Fe species in the hierarchical Fe-Beta.

Iron-based zeolites (mostly Fe-ZSM-5 and Fe-Beta) have been extensively investigated because of their high activity and thermal stability for the selective catalytic reduction of NO_x with NH_3 (NH_3-SCR) [1–6]. Compared with ZSM-5, Beta zeolite is an attractive host for iron and Fe-Beta zeolite has higher activity than Fe-ZSM-5 in some catalytic reactions [7,8]. Many studies focused on Fe-Beta catalysts for N_2O decomposition [8–11] and NH_3-SCR, especially on the active sites and hydrothermal stability [1,12,13]. Previous studies suggested that the low-temperature NH_3-SCR activity of Fe-Beta could be enhanced by bimetallic doping (such as Cu [14], Mn [15], Ce [16,17]) and high-temperature H_2-pretreatment [2,6].

Hierarchical zeolites contain both micro and meso-/macrospores, which can eliminate diffusion limitations and promote the accessibility of reactants to the active sites [18–21]. The predominant approach for the synthesis of hierarchical structure zeolites is demetallation (desiliconization and dealumination) and recrystallization with the surfactants [19,22]. Previous studies suggested that NH_3-SCR activity was enhanced by introducing hierarchical structure to Fe-ZSM-5 [23,24]. However, there are few open literatures about hierarchical Fe-Beta for NH_3-SCR.

In this work, hierarchical Fe-Beta zeolites catalysts were prepared by hydrothermal synthesis and evaluated for NH_3-SCR. The preparation procedure and activity tests are shown in the Support information. It was found that the low-temperature activity of hierarchical Fe-Beta was higher than that of Fe-Beta. The structure and activity relationship was discussed in detail.

As shown in Fig. 1, it was clear that the Beta was active for the SCR reaction in a narrow temperature range of 375–500 °C. Acidity may account for its catalytic performance [25,26]. Hierarchical Beta zeolite showed obviously improved NO conversions in the whole temperature range. This result indicated that hierarchical Beta zeolite may have more acid sites than Beta, which will be verified in the subsequent NH_3-TPD and NH_3 adsorption sections. After the doping of Fe, the Fe-Beta and hierarchical Fe-Beta indicated highly

* Corresponding author at: Ningbo Urban Environment Observation and Research Station-NUEORS, Institute of Urban Environment, Chinese Academy of Sciences, Ningbo 315800, China.
E-mail address: wpshan@iue.ac.cn (W. Shan).
[1] These two authors contributed equally to this work.

https://doi.org/10.1016/j.cclet.2019.03.011

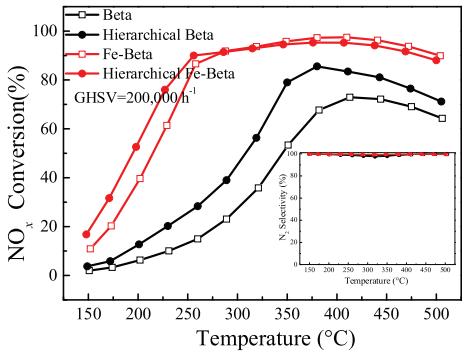

Fig. 1. NO_x conversion and N_2 selectivity (inserted) results of Fe-Beta and Beta catalysts. Reaction conditions: [NO] = [NH_3] =500 ppm, [O_2] =5 vol%, N_2 balance and GHSV = 200,000 h^{-1}.

improved SCR activity as compared with Beta and hierarchical Beta in the whole temperature of 150–500 °C. Hierarchical Fe-Beta showed enhanced low-temperature SCR activity compared with Fe-Beta obtained using the same ion-exchanged procedure. All of these catalysts presented excellent N_2 selectivity. The relationship of structure and activity was discussed in detail as follows.

The XRD patterns (Fig. S1 in Supporting information) show that all samples are phase-pure zeolites with the BEA framework structure. The peak intensity of Fe-Beta and hierarchical Fe-Beta declined, which may be due to the collapse or blocking of the partial microspore of zeolite. FeO_x species were not detected, which may be due to the Fe species existing as amorphous or high dispersion on the zeolite support [27,28].

The textural properties in Table S1 and Fig. S2 (Supporting information) show that the total volume, external surface area and BET surface area of hierarchical Beta are larger than those of Beta, indicating that mesopores and/or macropores are introduced into Beta to form hierarchical structure [19,20]. After doping with Fe, the BET surface area of both Fe-Beta and hierarchical Fe-Beta decreased, indicating that the partial microspore may be blocked, in agreement with the XRD results. ICP analysis revealed that the Fe content of Fe-Beta and hierarchical Fe-Beta was 2.82% and 3.71%, respectively, suggesting that hierarchical Fe-Beta could achieve a large amount of iron at the exchange sites under the identical ion-exchange procedure.

Comparing TEM images of hierarchical Fe-Beta (Figs. S3c and d in Supporting information) with those of Fe-Beta (Figs. S3a and b in Supporting information), the smaller crystal size and some hollow Beta structure were obtained during the hydrothermal synthesis, indicating the formation of micro-macroporous structure. This result is in accordance with the BET results. In Fig. S3c, the hollow zeolite was made of a polycrystalline micro-mesoporous shell and macropore core. Previous studies suggested that hollow Beta single crystals were much more difficult to prepare [18]. The absence of Al zoning prohibited the use of the dissolution-recrystallization strategy employing in the synthesis of hollow Beta zeolite single crystals [29].

UV-vis DR spectroscopy is an effective and common method for determining the nature and distribution of Fe species in Fe-zeolites. Fig. S4a (Supporting information) shows the UV–vis DR spectra of the Fe-Beta samples. The spectra were deconvoluted into sub-sands, which can be attributed to specific Fe species in the Fe-zeolites. The bands at 211 and 277 nm were respectively assigned to isolated Fe^{3+} ions in tetrahedral and octahedral coordination environments [30]. The bands at 300–400 nm indicated the presence of small oligomers $Fe_x^{3+}O_y$ in the zeolite channels [8,28], and the adsorption bands above 400 nm were attributed to the presence of bulky Fe_2O_3 nanoparticles on the external surface of the zeolite [31,32]. Fig. S4b (Supporting information) shows the UV–vis DR spectra of hierarchical Fe-Beta samples, the peak attributions are similar to Fe-Beta samples. The amount of Fe species was estimated semi-quantitatively based on the relative intensities of these sub-bands derived from UV–vis DR spectra and the total Fe loading in the zeolite. The data in Table S2 in Supporting information shows that isolated Fe^{3+} ions are the predominant species in Fe-Beta and hierarchical Fe-Beta catalysts. Previous studies suggested isolated Fe^{3+} species are active sites for NH_3-SCR on Fe-Beta catalysts [4,5,25,33,34]. When the Fe loadings were considered, the hierarchical Fe-Beta had the larger content of isolated Fe^{3+} species than Fe-Beta, resulted in the enhanced NH_3-SCR performance.

EPR spectroscopy was further employed to identify the nature of different Fe species, the corresponding results are illustrated in Fig. S5 (Supporting information). Signals at g = 2.0, g = 4.3 and g = 8.8 were observed for Fe-Beta and hierarchical Fe-Beta. The signals at g = 4.3, g = 8.8 and g = 2 were generally attributed to isolated Fe species in tetrahedral and distorted tetrahedral coordination [30,35], isolated Fe species with a distorted octahedral environment [8,13] and isolated Fe species in a high symmetry octahedral coordination or oligonuclear Fe_xO_y clusters [8,28], respectively. Overall, the EPR signal intensity of hierarchical Fe-Beta was higher than Fe-Beta, illustrating the amount of isolated Fe species on hierarchical Fe-Beta was higher than that of Fe-Beta, in agreement with UV–vis DRS results.

In order to investigate the redox performance of the samples, the H_2-TPR experiments were conducted and the results are shown in Fig. 2. There is no clear H_2 consumption signal for the Beta and hierarchical Beta. Two reduction peaks appeared on the Fe-Beta and hierarchical Fe-Beta. The overlapped reduction peaks centered at 354 °C (369 °C) and 441 °C (499 °C) were attributed to the reduction of isolated Fe^{3+} to Fe^{2+} [36] and oligomeric iron oxo species or tiny Fe_2O_3 into Fe_3O_4, respectively [37–39]. The reduction temperature of Fe species over hierarchical Fe-Beta was lower than Fe-Beta, which may be due to the better dispersion of Fe species. The amount of H_2 consumption of hierarchical Fe-Beta was larger than Fe-Beta, indicating that hierarchical Fe-Beta catalyst had more Fe active sites. The better redox performance resulted in the enhanced NH_3-SCR activity on the hierarchical Fe-Beta.

In view of the analysis of UV–vis DRS, EPR and H_2-TPR results above, we have confirmed that more Fe active species existed on the hierarchical Fe-Beta and dispersed better than those on Fe-Beta, which may be due to the specific hierarchical structure.

To identify the strength of the acid sites of hierarchical Fe-Beta, the NH_3-TPD experiments were carried out and the results are shown in Fig. 3. Beta zeolite showed NH_3 desorption peaks at the range of 100–500 °C, assigning to the desorption of ammonia species from weak Lewis acid sites (167 °C), strong Lewis acid sites (262 °C and 330 °C) and strong Brønsted acid sites (373 °C) [25,37,40]. The intensity of the desorption peak at 262 °C was much stronger than that of peak at 373 °C, suggesting that Beta zeolite had more Lewis acid sites because of its structural defects caused by the unsaturated bonding of silicon [41,42]. When

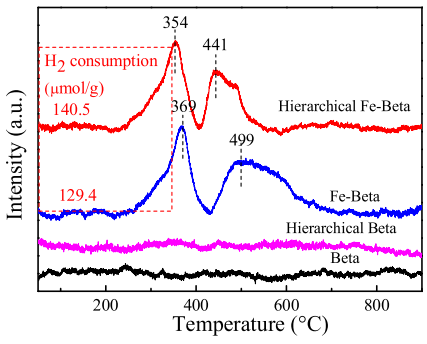

Fig. 2. H_2-TPR results of the different Beta samples.

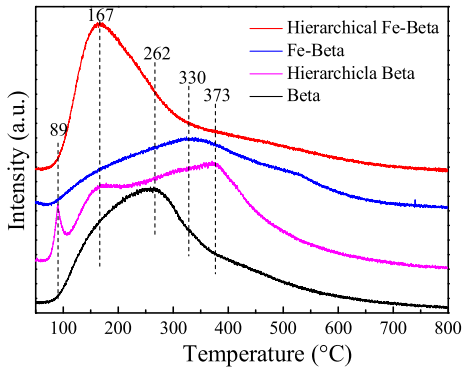

Fig. 3. NH_3-TPD profiles of different Beta zeolites.

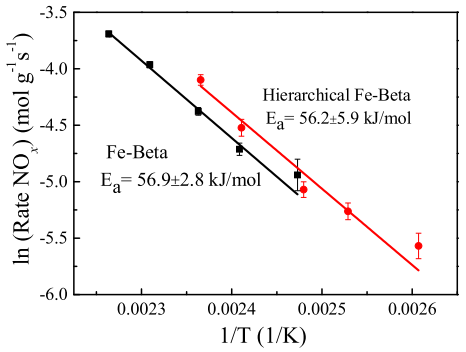

Fig. 4. Arrhenius plots of the SCR reaction rates over Fe-Beta and hierarchical Fe-Beta in the feed gas of 500 ppm NO/ 500 ppm NH_3/ 5.0% vol% O_2/ N_2 (500 mL/min, 40 mg catalysts, GHSV: 400,000 h^{-1}).

forming the hierarchical structure, the peaks shifted to the high-temperature, demonstrating the formation of the stronger acid sites. The peak at 89 °C on hierarchical Beta may be attributed to physisorbed NH_3 [39,43]. The number of acid sites of hierarchical Beta also increased, which resulted in the enhanced SCR activity, compared with Beta zeolite (Fig. 1). When Fe was introduced into Beta, the NH_3 storage capacity decreased, and the desorption peak shifted to high-temperature. However, when Fe was exchanged to hierarchical Beta, the NH_3 desorption peak shifted to the low-temperature, to form more weak Lewis acid sites (167 °C), which is beneficial to the adsorption and activation of NH_3.

In order to understand the adsorption performance and reaction mechanism, in situ DRIFTS experiments were carried out for Fe-Beta and hierarchical Fe-Beta (Fig. S6 in Supporting information). After the adsorption of NH_3 and N_2 purge, the NH_3 adsorbed peaks appeared on both of the catalysts. The negative bands at 3773, 3721, 3604 cm^{-1} was assigned to Al-OH groups, terminal Si-OH, isolated bridging acidic hydroxyl stretching vibrations (Si(OH)Al), respectively [44–46]. The negative band at 3675 cm^{-1} only appeared on hierarchical Fe-Beta, which was attributed to hydroxyls bonded on extra-framework Al species [47], due to hierarchical structure. This result indicated that hierarchical structure introduced more exchanged sites and acid sites, which led to the better SCR activity. In the N-H stretching regions (3100-3500 cm^{-1}), the bands corresponding to the asymmetric stretching (3343 cm^{-1}) and symmetric stretching (3273 and 3192 cm^{-1}) of coordinated NH_3 on Lewis acid sites were observed, respectively [48]. The bands at 1478 cm^{-1} and 1163 cm^{-1} were attributed to the NH_4^+ ions adsorbed on the Brønsted acid sites and coordinated NH_3 adsorbed on the Lewis acid sites, respectively [48–50]. The band at 896 cm^{-1} could be assigned to T-O-T framework vibrations by Fe species [7]. The peak intensity at 896 cm^{-1} of hierarchical Fe-Beta was higher than that of Fe-Beta, illustrating more Fe was incorporated into hierarchical Fe-Beta, in agreement with the ICP, EPR and H_2-TPR results. Overall, the intensity of NH_3 adsorption peaks for hierarchical Fe-Beta was higher than those for Fe-Beta, suggesting more acid sites existing on hierarchical Fe-Beta than those on Fe-Beta, in accordance with NH_3-TPD results.

The NO adsorbed spectra were shown in Fig. S6b. No peak for NO_x adsorbed species was clearly observed, suggesting that Fe-Beta and hierarchical Fe-Beta did not adsorb NO_x species. The NO_x adsorbed species were not detected on the Fe-Beta and hierarchical Fe-Beta, but the excellent NO_x conversion could be obtained, illustrating that the NH_3-SCR reaction may mainly carried out through Eley-Rideal (E-R) pathway with gaseous NO reacting with adsorbed NH_3 species on both of the catalysts.

In order to obtain further understanding of the intrinsic effect of hierarchical structure on the NH_3-SCR reaction, the kinetic experiments were performed on the Fe-Beta and hierarchical Fe-Beta, as shown in Fig. 4. The apparent activation energy obtained from the Arrhenius plots for Fe-Beta and hierarchical Fe-Beta was 56.9 and 56.2 kJ/mol, respectively, in agreement with those for Fe-zeolite reported in the previous literature (Ea = 40∼54 kJ/mol) [31,51,52]. The two catalysts had similar activation energy, indicating an identical rate controlling mechanism [13]. Since there were no mass transfer related limitations, hierarchical Fe-Beta catalyst had better SCR activity, demonstrating the higher activity was mainly caused by higher amount of Fe active sites [53], in accordance with the H_2-TPR and UV–vis DRS results.

In summary, hierarchical Beta was prepared by hydrothermal synthesis. The BET and TEM results confirmed that the meso/macrospores were introduced to Beta zeolite. Hierarchical Fe-Beta exhibited better low-temperature activity than Fe-Beta. The results of UV–vis DRS, EPR and H_2-TPR indicated that isolated Fe^{3+}, oligomers and Fe_2O_3 coexisted on Fe-Beta and hierarchical Fe-Beta. The enhanced activity of the hierarchical Fe-Beta was related to the prominent presence of highly dispersed Fe active species, which may be because that the hierarchical structure introduced more defects to provide more ion-exchange sites for Fe species. The kinetic experiments demonstrated that the activate energy of Fe-Beta and hierarchical Fe-Beta was 56.2 and 56.9 kJ/mol, respectively, suggesting an identical rate controlling mechanism. The NH_3-TPD and DRIFTS results of NH_3 adsorption indicated that the hierarchical Fe-Beta had more acid sites for the adsorption and activation of NH_3. The adsorption of NO_x was not clearly observed on Fe-Beta or hierarchical Fe-Beta, indicating that NH_3-SCR process of both of the two catalysts mainly followed the Eley-Rideal (E-R) reaction mechanism.

Acknowledgments

We gratefully acknowledge the financial supports from the National Natural Science Foundation of China (Nos. 51822811, 21637005), the National Key R&D Program of China (Nos. 2017YFC0212502, 2017YFC0211101), and the Young Talent Project of the Center for Excellence in Regional Atmospheric Environment, CAS (No. CERAE201806).

Appendix A. Supplementary data

Supplementary material related to this article can be found, in the online version, at doi:https://doi.org/10.1016/j.cclet.2019.03.011.

References

[1] S. Shwan, R. Nedyalkova, J. Jansson, et al., Ind. Eng. Chem. Res. 51 (2012) 12762–12772.
[2] R. Nedyalkova, S. Shwan, M. Skoglundh, L. Olsson, Appl. Catal. B: Environ. 138 (2013) 373–380.
[3] H. Chen, W.M.H. Sachtler, Catal. Today 42 (1998) 73–83.

[4] P. Balle, B. Geiger, D. Klukowski, et al., Appl. Catal. B: Environ. 91 (2009) 587–595.
[5] P. Balle, B. Geiger, S. Kureti, Appl. Catal. B: Environ. 85 (2009) 109–119.
[6] S. Shwan, J. Jansson, L. Olsson, M. Skoglundh, Catal. Sci. Technol. 4 (2014) 2932–2937.
[7] M. Mauvezin, G. Delahay, B. Coq, et al., J. Phys. Chem. B 105 (2001) 928–935.
[8] J. Perez-Ramirez, J.C. Groen, A. Bruckner, et al., J. Catal. 232 (2005) 318–334.
[9] J.A.Z. Pieterse, G.D. Pirngruber, J.A. van Bokhoven, S. Booneveld, Appl. Catal. B: Environ. 71 (2007) 16–22.
[10] K. Jisa, J. Novakova, M. Schwarze, et al., J. Catal. 262 (2009) 27–34.
[11] S. Sklenak, P.C. Andrikopoulos, B. Boekfa, et al., J. Catal. 272 (2010) 262–274.
[12] S. Shwan, R. Nedyalkova, J. Jansson, et al., Top. Catal. 56 (2013) 80–88.
[13] H. Liu, J. Wang, T. Yu, S. Fan, M. Shen, Catal. Sci. Technol. 4 (2014) 1350–1356.
[14] L. Xu, C. Shi, B. Chen, et al., Microporous Mesoporous Mater. 236 (2016) 211–217.
[15] D.S. Krivoruchenko, A.V. Kucherov, N.S. Telegina, et al., Russ. Chem. Bull. 63 (2014) 389–395.
[16] S. Jiang, R. Zhou, Fuel Process. Technol. 133 (2015) 220–226.
[17] J. Li, L. Jia, W. Jin, F. Xia, J. Wang, Rare Metal Mater. Eng. 44 (2015) 1612–1616.
[18] C. Pagis, A.R.M. Prates, D. Farrusseng, N. Bats, A. Tuel, Chem. Mater. 28 (2016) 5205–5223.
[19] E. Koohsaryan, M. Anbia, Chin. J. Catal. 37 (2016) 447–467.
[20] L. Chen, X. Li, J.C. Rooke, et al., J. Mat. Chem. 22 (2012) 17381–17403.
[21] F. Xiao, L. Wang, C. Yin, et al., Angew. Chem. Int. Ed. 45 (2006) 3090–3093.
[22] K. Na, M. Choi, R. Ryoo, Microporous Mesoporous Mater. 166 (2013) 3–19.
[23] P.N.R. Vennestrom, M. Grill, M. Kustova, et al., Catal. Today 168 (2011) 71–79.
[24] J. Ma, D. Weng, X. Wu, Z. Si, Z. Wu, Prog. Nat. Sci. 23 (2013) 493–500.
[25] L. Ma, H. Chang, S. Yang, et al., Chem. Eng. J. 209 (2012) 652–660.
[26] Y. Zhu, B. Chen, R. Zhao, et al., Catal. Sci. Technol. 6 (2016) 6581–6592.
[27] M. Jablonska, G. Delahay, K. Kruczala, et al., J. Phys. Chem. C 120 (2016) 16831–16842.
[28] H. Xia, H. Hu, S. Xu, K. Xiao, S. Zuo, Biomass Bioenergy 108 (2018) 426–432.
[29] A.R.M. Prates, C. Pagis, F.C. Meunier, et al., Cryst. Growth Des. 18 (2018) 592–596.
[30] A. Wang, Y. Wang, E.D. Walter, et al., J. Catal. 358 (2018) 199–210.
[31] S. Brandenberger, O. Krocher, A. Tissler, R. Althoff, Appl. Catal. B: Environ. 95 (2010) 348–357.
[32] M.S. Kumar, M. Schwidder, W. Grunert, A. Bruckner, J. Catal. 227 (2004) 384–397.
[33] D.E. Doronkin, A.Y. Stakheev, A.V. Kucherov, et al., Top. Catal. 52 (2009) 1728–1733.
[34] M. Hoj, M.J. Beier, J.D. Grunwaldt, S. Dahl, Appl. Catal. B: Environ. 93 (2009) 166–176.
[35] M.Y. Kim, K.W. Lee, J.H. Park, et al., Korean J. Chem. Eng. 27 (2010) 76–82.
[36] R.Q. Long, R.T. Yang, J. Catal. 194 (2000) 80–90.
[37] Y. Xia, W. Zhan, Y. Guo, Y. Guo, G. Lu, Chin. J. Catal. 37 (2016) 2069–2078.
[38] H. Pan, Y. Guo, H. Bi, Chem. Eng. J. 280 (2015) 66–73.
[39] L. Ma, J. Li, H. Arandiyan, et al., Catal. Today 184 (2012) 145–152.
[40] L. Xu, C. Shi, Z. Zhang, et al., Microporous Mesoporous Mater. 200 (2014) 304–310.
[41] P. Boron, L. Chmielarz, J. Gurgul, et al., Microporous Mesoporous Mater. 203 (2015) 73–85.
[42] Q. Zeng, X. Bai, J. Zheng, J. Chen, R. Li, Chin. Chem. Lett. 22 (2011) 1103–1106.
[43] S. Yang, J. Li, C. Wang, et al., Appl. Catal. B: Environ. 117 (2012) 73–80.
[44] J.H. Baek, S.M. Lee, J.H. Park, et al., J. Ind. Eng. Chem. 48 (2017) 194–201.
[45] S. Shwan, E.C. Adams, J. Jansson, M. Skoglundh, Catal. Lett. 143 (2013) 43–48.
[46] W. Su, H. Chang, Y. Peng, C. Zhang, J. Li, Environ. Sci. Technol. 49 (2015) 467–473.
[47] E. Bourgeat-Lami, P. Massiani, F.D. Renzo, et al., Appl. Catal. A Gen. 72 (1991) 139–152.
[48] S. Song, G. Wu, W. Dai, N. Guan, L. Li, Catal. Sci. Technol. 6 (2016) 8325–8335.
[49] S.A. Skarlis, D. Berthout, A. Nicolle, C. Dujardin, P. Granger, J. Phys. Chem. C 117 (2013) 7154–7169.
[50] Y. Peng, W. Yu, W. Su, X. Huang, J. Li, Catal. Today 242 (2015) 300–307.
[51] H. Huang, R.Q. Long, R.T. Yang, Appl. Catal. A: Gen. 235 (2002) 241–251.
[52] P. Sazama, B. Wichterlova, S. Sklenak, et al., J. Catal. 318 (2014) 22–33.
[53] I. Melian-Cabrera, E.R.H. van Eck, S. Espinosa, et al., Appl. Catal. B: Environ. 203 (2017) 218–226.